

SIMPLIFIED FAILURE MODE MAPS FOR SANDWICH BEAMS

Mondal, A.¹ and Nakhla, S. *²

¹Graduate Student, ²Assistant Professor

Mechanical Engineering Department

Faculty of Engineering and Applied Science,

Memorial University of Newfoundland, St. John's, NL, Canada

*Corresponding author (satnakhla@mun.ca)

Keywords: *Failure, Sandwich, Analysis*

ABSTRACT

Failure modes of composite sandwich beams are outlined. Simplified theoretical predictions based on Euler-Bernoulli beam theory are introduced and discussed. Theoretical predictions are compared with other analytical models in open literature. Further comparisons are held with test data available in literature. These comparisons concluded sufficiently accurate predictions from simplified models. Finally, failure mode maps are constructed through consistent non-dimensionalization of geometric and material parameters extending the applicability of failure mode maps to provide useful design tool.

1 INTRODUCTION

The use of sandwich panels mostly increased after World War II [1]. Since then sandwich panels are becoming increasingly popular in sectors where high stiffness-to-weight ratio is necessary such as aerospace and marine industries. The work of Plantema [1] and Allen [2] focused on analysis of sandwich panels in terms of their stiffness and strength while further work in literature [3–6] focused on their failure mechanisms. These failure mechanisms can be associated to either one of the sandwich panel components, i.e. facesheet or core. For example, Plantema [1] and Allen [2] presented discussions on sandwich panels buckling under in-plane loading. These discussions clarify the crucial aspects of buckling failure in which a facesheet debonds from the core. Facesheet debonding can occur in either one of two ways. Complete debonding of the face from core which is also known as global buckling. Alternatively a partial debonding may occur between face and core which is known as local buckling or facesheet wrinkling. Carlson and Kardomateas [3], Niu and Talreja [4] and Mondal and Nakhla [5] studied facesheet debonding failure in various loading scenarios. Various analytical approaches were used in [3–5] to develop expressions for local buckling load conditions in sandwich panels. Isaac Daniel et al. [6] developed a detailed investigation of failure modes in sandwich composite beams and their associated prediction criteria. In their investigation they highlighted the dependency of failure modes on material properties and geometry of facesheets and core as well as loading conditions. They also stressed on the essential need to carefully conduct experiments on these beams to accurately delineate the conditions leading to failure. Also in [6] they outlined the failure modes in sandwich panels to be facesheet failure, core failure, global buckling, wrinkling and indentation failure under concentrated load. Facesheet failure is explained to be due to uniaxial tensile or compressive stress, while the core commonly fails due to shear stresses [2]. Kim and Swanson [7], Gibson et al. [8], Kabir et al. [9] have shown in their experimental studies how the core of a sandwich panel fails in shear. Whereas facesheet debonding due to manufacturing defects or impact loading reduces panel stiffness and increases the potential of occurrence of global

SIMPLIFIED FAILURE MODE MAPS FOR SANDWICH BEAMS

buckling [6]. Facesheet wrinkling also known as short wavelength buckling is mainly governed by the through-the-thickness direction core modulus. Finally, indentation failure takes place when external loads result in local yield of core associated with significant local deformation of the facesheet into the core. For example, a three-point bending test conducted without reinforcing the facesheet under the load application points. In order to enhance the understanding of failure modes in sandwich panels many researchers developed failure mode maps. Petras and Sutcliffe [10] constructed failure mode maps for facesheet failure, core shear, core crushing and wrinkling as a function of relative density and thickness of the facesheet. Shenhar et al. [11] and Steeves and Fleck [12] also presented failure mode maps for sandwich panels. Steeves and Fleck [12] constructed failure mode maps for microbuckling, wrinkling, core shear and indentation failure to deduce the aspect ratio of the facesheet and the core.

In the current study simple analytical models are used to present an effective methodology to construct the failure maps of sandwich panels for the purpose of design optimization. Special attention is paid to the wrinkling failure mode to derive its analytical model based on the classical approach of Winkler foundation. Also other analytical solutions for facesheet compressive failure, core shear failure, buckling and wrinkling are presented. All presented or developed analytical solutions are compared with test data and other analytical predictions available in literature. Non-dimensional failure maps are constructed for failure modes generating contour plots of failure modes as a function of non-dimensional core and facesheet thickness. Therefore, non-dimensional failure mode maps are made useful to select facesheet and core materials based on their respective geometries and material properties. Also, for the purpose of weight minimization, non-dimensional mass of the sandwich is incorporated into failure mode map.

2 ANALYSIS

This section aims at discussing simplified models to predict sandwich panel failure modes. For this purpose, a unified formulation based on Euler-Bernoulli (E-B) beam theory is used. Failure modes discussed in this section are facesheet failure, core failure, global buckling and wrinkling of facesheet. A general problem of a simply supported sandwich panel is used throughout the analysis. The panel is under distributed load $q(x)$ and distributed moment $m(x)$ as illustrated in Figure 1. The detailed geometry of the cross section is shown in Figure 2. For the purpose of comparison with test data, numerical predictions developed within are compared to test results documented in [6]. Carbon/epoxy (AS4/3501-6) and PVC foam Divinycell H250 are generally used for facesheet and foam core, respectively, unless otherwise mentioned. The material properties of these constituents and panel geometry are adopted from [6] and provided in Table 1.

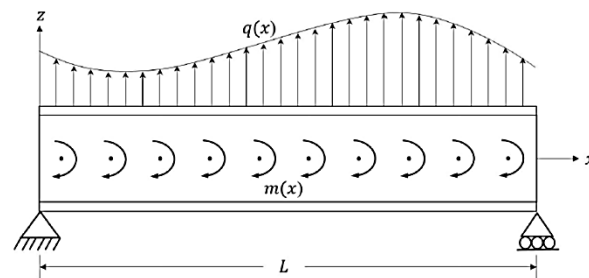


Figure 1. Simply supported sandwich beam under distributed load and moment

SIMPLIFIED FAILURE MODE MAPS FOR SANDWICH BEAMS

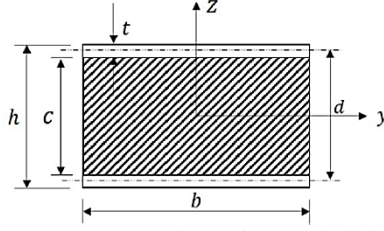


Figure 2: Cross-section of a sandwich beam

Property	Carbon/Epoxy	Foam H250
Density (kg/m^3)	$\rho_f = 1620$	$\rho_c = 250$
Young's Modulus (GPa)	$E_f = 147$	$E_c = 0.403$
Shear Modulus (GPa)	–	$G_c = 0.117$
Poisson's Ratio	$\nu_f = 0.25$	$\nu_c = 0.32$
Compressive Strength (MPa)	$\sigma_{all} = 1930$	–
Shear Strength (MPa)	–	$\tau_{all} = 5$
Thickness (mm)	$t = 0.8$	$c = 25.4$
Width (mm)	$b = 26$	
Length (mm)	$L = 406$	

Table 1. Geometric and Material Properties of sandwich panel constituents [6]

2.1 Normal Stress in the facesheet

As expressed by Daniel et al. [6] uniaxial stresses, tensile or compressive is responsible for facesheet failure. This can be explained by realizing that the facesheet is responsible for carrying normal stresses due to its increased normal stiffness in comparison to the soft core material. In [6] they recorded their observation by testing a sandwich panel with carbon/epoxy face and aluminum honeycomb core. They explained the observed failure to be dominantly the result of compressive stresses in the face. Moreover they concluded the adequacy of linear bending theory to predict facesheet failure. Consequently in this section the normal stress in the facesheet is predicted using Euler-Bernoulli beam theory for built-up sections as explained in Gere [13]

$$\sigma_f = \frac{E_f M z}{E_f I_f + E_c I_c} \quad (1)$$

where, M is the maximum moment at the cross-section, E_f and E_c are the homogenized moduli of the facesheet and core, respectively, and I_f and I_c are the second moment of area of the face and core, respectively obtained at the panel midplane. The homogenized modulus of the facesheet, E_f can be obtained using the extensional stiffness matrix A as demonstrated by Mallick [14]. The facesheet is assumed to be symmetric around its own mid-plane to guarantee hygrothermal stability, hence

$$A = \begin{bmatrix} A_{11} & A_{12} & 0 \\ A_{12} & A_{22} & 0 \\ 0 & 0 & A_{33} \end{bmatrix} \quad (2)$$

The homogenized modulus E_f can be expressed as

$$E_f = \frac{A_{11}A_{22} - A_{12}^2}{tA_{22}} \quad (3)$$

In the four-point bending test of a sandwich panel conducted by Daniel et al. [6] compressive failure of facesheet was observed to occur at an applied moment of 1.09kN.m. The calculated compressive stress in the facesheet using Equation (1) is 2061MPa where the compressive strength of carbon/epoxy facesheet is 1930MPa. The percentage

difference between calculated compressive stress in the facesheet and its failure strength is 6.8%. Therefore, the expression in Equation (1) provides sufficiently accurate prediction of the facesheet compressive failure.

2.2 Shear Stress in the core

Contrary to normal stresses the core of a sandwich panel is responsible for carrying shear stresses [6]. Allen [2] modified the shear stress equation based on E-B beam theory to account for a beam of compound cross-section

$$\tau = \frac{V}{EI_{eq}b} \sum QE \quad (4)$$

where, V is the maximum shear force, EI_{eq} is the total bending stiffness of the sandwich, b is its width and the summation term is carried out over the product of the first moment of area Q and the corresponding modulus E of section constituents. Allen [2] also explained that the shear stress is maximum at the mid-plane of the sandwich panel, if symmetric. Therefore, Equation (4) can be expressed at the mid-plane as

$$\tau = \frac{V}{EI_{eq}b} \left(\frac{E_f t d}{2} + \frac{E_c c^2}{8} \right) \quad (4)$$

where,

$$EI_{eq} = E_f I_f + E_c I_c \quad (5)$$

Daniel et al. [6] documented that shear failure occurs in the vicinity of the proportional limit of the shear stress-strain curve of the core. Therefore, shear stress failure can simply be predicted using Equation (5). Other researchers developed further solutions to enhance the accuracy of shear stress prediction in the core. For example, Steeves and Fleck [12] elected to use the nonlinear solution developed by Chiras et al. [15] to predict the shear stress in a sandwich panel. This nonlinear solution is based on Timoshenko beam theory for the case of rigid-ideally plastic core and elastic facesheets. The expression developed by Chiras et al. [15] is

$$\tau_c = \frac{2V - 8E_f b(t/L)^3 \delta}{2bd} \quad (7)$$

where,

$$\delta = \frac{2VL^3}{48EI_{eq}} + \frac{2VL}{4AG_{eq}} \quad (8)$$

where, AG_{eq} is the total shear rigidity of the sandwich panel which can be approximated as the shear rigidity of the core material. A three point bending test was conducted by Daniel et al. [6]. The span length of the panel was 380mm. They documented that non-uniform shear deformation starts close to the proportional limit of the stress-strain curve of the H250 foam which is 2.55 MPa. For this case, the predicted shear stress in the core using Equation (5) and (7) are 2.47 MPa and 2.42 MPa, respectively. The percentage differences of the predicted shear stress in the foam are -3% and -5.1%, respectively. Therefore, E-B beam theory provides sufficiently accurate prediction to the onset of shear failure

2.3 Facesheet Debonding

A sandwich panel is constructed by adhesively bonding two thin facesheets on both sides of a soft core material; hence there exists the possibility of facesheet debonding from core during load application. Facesheet debonding may occur due to fabrication imperfections in the sandwich panel or external impact loading. Debonding results in the reduction of facesheet bending stiffness. As stated earlier, buckling of the facesheet can be global or local and alternatively referred to as global buckling and wrinkling, respectively. Many researchers have developed expressions to predict the buckling and wrinkling loads for a sandwich panel using various methods.

2.3.1 Global Buckling

Bauchau and Craig [16] provide an expression to predict global buckling load by idealizing the facesheet as a simply supported beam resting on an elastic foundation as shown in Figure 3. The stiffness of the elastic foundation is defined in terms of the transverse modulus of the core, E_c . For this purpose, they demonstrate using the Principle of Minimum Total Potential Energy (PMTPE) based on E-B beam theory.

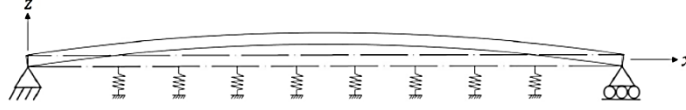


Figure 3. Idealised facesheet in global buckling

The global buckling load as provided in [16] is expressed in terms of a wave number, n , as

$$P_b = \frac{n^2 \pi^2 E_f b t^3}{12 L^3} + \frac{E_c L^2}{n^2 \pi^2} \tag{9}$$

In [16] they identified the minimum global buckling load to correspond to a wave number of unity. Meanwhile, in the tests conducted by Daniel et al. [6] no global buckling was observed in the absence of manufacturing imperfections and impact damage. In other words, this failure mode is triggered by initial imperfections or damage. Therefore, theoretical values of global buckling load will be used within without comparison with test data

2.3.2 Wrinkling (Local Buckling)

There exists in literature a number of expressions to predict facesheet wrinkling load. Hoff and Mautner derived an expression, as explained by Carlson and Kardamatas [3], using a linear decay function. Plantema [1], Allen [2] and Niu and Talreja [4] also established expressions to predict the minimum wrinkling load. Recently, Mondal and Nakhla [5] developed an expression based on E-B beam theory using PMTPE and the classical approach of Winkler foundation. This approach is consistent with the one provided in Bauchau and Craig [16] for global buckling. Face wrinkling is characterized by local instabilities, as shown in Figure 4, possessing shorter wavelength than those in global buckling. In order to develop a mathematical model for wrinkling both displacement and slope are assumed to be zero at the boundaries of the wrinkling length. Therefore, wrinkling of facesheet can be idealized as a beam resting on elastic foundation as shown earlier in Figure 3.

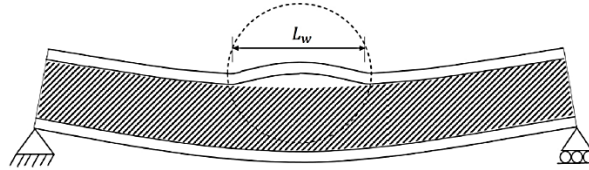


Figure 4. Wrinkling of the top facesheet

The wrinkled length L_w of the beam is considered for the analysis, where $L_w = \alpha L$ ($0 < \alpha < 1$). The bending stiffness of the facesheet is

$$H_f = E_f I_{f_0} \tag{10}$$

where I_{f_0} is the second moment of area of the facesheet around its own local centroid or mid-plane. To utilize the PMTPE approach the displacement field is assumed to be

$$w(x) = a(\xi^2 - 2\xi^3 + \xi^4) \tag{11}$$

where $\xi = x/L$ and a is an unknown displacement parameter. This function satisfies all essential boundary conditions of the differential equation. Total potential energy of the system Π is the superposition of strain energies

SIMPLIFIED FAILURE MODE MAPS FOR SANDWICH BEAMS

due to the bending of the facesheet, strain energy in the elastic foundation (the core) and potential energy of the applied load, P

$$\Pi = \frac{1}{2} \int_0^{L_w} H_f \left(\frac{d^2w}{dx^2} \right)^2 dx + \frac{1}{2} \int_0^{L_w} E_c w^2 dx - \frac{1}{2} \int_0^{L_w} P \left(\frac{dw}{dx} \right)^2 dx \quad (12)$$

Substituting the assumed displacements into (12) and integrating

$$\Pi = H_f \frac{2a^2}{5L_w^3} + E_c \frac{L_w a^2}{1260} - P \frac{a^2}{105L_w} \quad (13)$$

The total potential energy is expressed here as a function of the unknown amplitude a . Applying the PMTPE theory

$$\frac{d\Pi}{da} = \left(H_f \frac{4}{5L_w^3} + E_c \frac{L_w}{630} - P \frac{2}{105L_w} \right) a = 0 \quad (14)$$

Either a is zero or the term in parenthesis is zero. In the latter case, $P = P_w$ is the load at which wrinkling of the facesheet occurs

$$P_w = H_f \frac{42}{L_w^2} + E_c \frac{L_w^2}{12} \quad (15)$$

An expression for the wrinkling length can be obtained by differentiating Equation (15) with respect to the length L_w . The expression for the minimum value of wavelength L_w that corresponds to minimum P_w is

$$L_w = \sqrt[4]{504H_f/E_c} \quad (16)$$

Equation (16) can be substituted back into (15) to write an expression for the minimum wrinkling load in the facesheet. The expressions developed by Hoff and Mautner (as documented in Carlson and Kardomateas [3]), Plantema [1], Allen [2] and Niu and Talreja [4] are provided in Equations (17), (18), (19) and (20), respectively. Niu and Talreja [4] developed expressions for short and long wavelength wrinkling. For the purpose of comparisons with test data provided in [6] only the short wavelength expression from [4] is applicable and provided in Equation (20).

$$P_{Hoff} = 0.91 bt \sqrt[3]{E_f E_c G_c} \quad (17)$$

$$P_{Allen} = bt B_1 \sqrt[3]{E_f E_c^2} \quad (18)$$

where $B_1 = 3[12(3 - \nu_c)^2(1 + \nu_c)^2]^{-1/3}$

$$P_{Hoff} = 0.825 bt \sqrt[3]{E_f E_c G_c} \quad (19)$$

$$P_{Talreja} = bt \left[\left(\frac{3E_c}{2(1+\nu_c)(3-\nu_c)} \right)^{2/3} E_f^{1/3} + \frac{(1-\nu_c)E_c}{2(1+\nu_c)(3-\nu_c)} + \left(\frac{3E_c}{(1+\nu_c)(3-\nu_c)} \right)^{4/3} \left(\frac{3}{2E_f} \right)^{1/3} \right] \quad (20)$$

In two four-point-bending tests conducted by Daniel et al. [6] wrinkling of the facesheet was observed for foam core sandwich panels. They reported their observations and concluded that wrinkling behavior is controlled by the core modulus. In a four-point bending test of a sandwich panel with Divinycell H100 foam core they measured a critical wrinkling load of 14 kN. A comparison is held between analytical predictions and the measured wrinkling load as recorded in [6]. The results from this comparison are provided in Table 2. Comparing the predicted values for wrinkling load in Table 2, it can be noticed that current method is consistent with other analytical models in terms of accuracy. Also all analytically developed solutions over predict the wrinkling load.

A	Wrinkling Load in kN Percentage comparison with [6]
Current	17.8 (%27.1)
Hoff and Mautner [3]	18.8 (%34.3)
Allen [2]	16.6 (%18.6)
Plantema [1]	17.0 (%21.4)
Niu and Talreja [4]	17.2 (%22.9)

Table 2. Comparison of predicted wrinkling load from analytical methods

3 FAILURE MODE MAPS

In this section failure mode maps are constructed for different failure modes discussed in the previous section. Using E-B beam theory as the unified basis for constructing these maps guarantees consistent and straight forward approach. Also, consistent non- dimensional parameters are used while constructing these maps for the same purpose of unified basis. Moreover, the knowledge gained in comparing analytical predictions with test results from [6] is introduced into the developed maps. Finally, the constructed maps are discussed and proposed as a design tool for sandwich construction. Non-dimensional parameters are defined based on material properties and geometry of the sandwich panel constituents. Allowable values for facesheet normal stress and core shear stress are used to obtain the non-dimensional failure modes of facesheet and core materials, respectively. While Euler buckling loads for simply supported and clamped-clamped beams are used for global buckling and wrinkling of the facesheet, respectively. Finally, the total thickness h , of the sandwich is used to non-dimensionalize the geometry of the cross-section. Therefore, non-dimensional geometry of the cross section and length of the sandwich panel can be expressed as

$$\bar{t} = t/h; \bar{c} = c/h; \bar{b} = b/h; \bar{L} = L/h; \bar{E} = E_c/E_f \quad (21)$$

Non-dimensional normal stress in the facesheet is obtained from Equation (1)

$$\bar{\sigma} = \bar{M} \frac{3\bar{t}(\bar{c}+\bar{t})}{6\bar{t}(\bar{c}+\bar{t})^2 + \bar{E}\bar{c}^3} \quad (22)$$

where the non-dimensional bending moment is $\bar{M} = M/(\sigma_{all}bt(d/2))$.

Non-dimensional shear stress in the core is obtained from Equation (5)

$$\bar{\tau} = \bar{V} \left[\frac{\bar{c}}{\bar{c}+\bar{t}} + \frac{\bar{E}}{4} \frac{\bar{c}^3}{\bar{t}(\bar{c}+\bar{t})^2} \right] \quad (23)$$

where $\bar{V} = V/(\tau_{all}bt)$.

Non-dimensional global buckling load of the facesheet is obtained from Equation (9)

$$\bar{P}_b = 1 + \frac{12\bar{E}\bar{L}^4}{\pi^4\bar{b}\bar{t}^3} \quad (24)$$

Non-dimensional wrinkling load of the facesheet is obtained from Equation (15).

$$\bar{P}_w = 0.6161 \sqrt{\frac{\bar{E}\bar{L}^4}{\bar{b}\bar{t}^3}} \quad (25)$$

Using the properties of carbon/epoxy facesheet and H250 foam core given in Table 1 the following failure mode maps are constructed. Failure mode maps of non-dimensional normal and shear stress are constructed from Equation (22) and (23). The failure mode maps for normal and shear stresses are shown in Figure 5. In Figure 5 the values on contour lines denotes the values of non-dimensional stresses. For example, a solid line with a value of unity indicates that along this line the normal stress in the facesheet is equal to the allowable stress of the facesheet. For design purpose, the value of \bar{t} and \bar{c} should be such that contour lines has a value less than unity as this indicates stresses being lower than their corresponding allowable values. Non-dimensional global buckling and wrinkling load are plotted in Figure 6. From Figure 6 it is noticeable that global buckling load is higher than wrinkling load. This indicates that wrinkling failure is more likely to occur before buckling. This is also verified by the experiments conducted by Daniel et al. [6] where wrinkling is observed in foam core sandwich panels while no global debonding of the facesheet took place. Therefore, wrinkling should be considered more critical than buckling while designing a sandwich panel. Figure 6 also indicates that the buckling and wrinkling behaviors are mainly dependent on the facesheet non-dimensional thickness rather than that of the core. Moduli ratio of constituents \bar{E} is used to construct Figure 7 to investigate the effect of constituents' selection on buckling and wrinkling loads. Figure 7 clearly shows that the softer the core material becomes the higher susceptibility to buckling and wrinkling failure

SIMPLIFIED FAILURE MODE MAPS FOR SANDWICH BEAMS

Sandwich panel can be optimized by minimizing the mass of the panel. If the density of the facesheet and the core is ρ_f and ρ_c , respectively, then the mass of a sandwich panel m_s is the sum of the facesheets mass m_f and that of the core m_c

$$m_s = m_f + m_c \quad (26)$$

where $m_f = 2bLt\rho_f$ and $m_c = bLc\rho_c$. Non-dimensional mass of the panel is obtained from Equation (26).

$$\bar{m} = \frac{m_s}{bLh\rho_f} = 2\bar{t} + \bar{c}\bar{\rho} \quad (27)$$

where $\bar{\rho}$ is a nondimensional density parameter $\bar{\rho} = \rho_c/\rho_f$. Equation (27) is plotted in Figure 8 along with the non-dimensional normal and shear failure mode maps. Figure 8 shows that the thickness of the facesheet has higher contribution over the mass of the sandwich panel than the thickness of the core. Figure 8 suggests that the thickness of the facesheet should be kept low for designing a lightweight sandwich panel. Figures 7 and 8 represent useful tools for the designer to make design selections. Figure 7 can be used to select the material properties of constituents leading to the choice of non-dimensional facesheet thickness. Then Figure 8 can be utilized to select non-dimensional core thickness leading to cross-sectional geometry determination. This process can be repeated till a final selection is fully realized for optimal structural performance and minimum weight of sandwich.

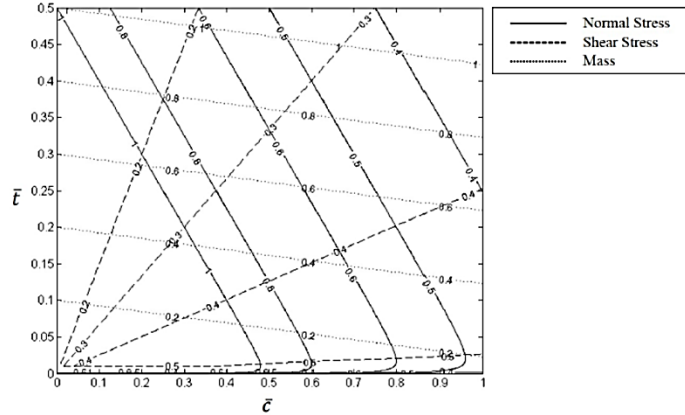


Figure 8. Failure mode maps for non-dimensional normal and shear stresses with non-dimensional mass

4 DISCUSSION AND CONCLUSION

A general discussion of failure modes of sandwich beams is presented for the purpose of arriving at unified basis. Euler-Bernoulli beam theory and the classical approach of Winkler foundation are used as the unified basis. A special attention is made to develop a simplified model for wrinkling failure. The developed model utilizes beam theory and Winkler foundation approach within the framework of the PMTPE. The developed wrinkling failure model is in good agreement with other analytical solutions published in literature. Additionally all analytical predictions of presented failure modes are compared to test data and other analytical solutions available in literature. Comparisons prove adequate predictions of all simplified failure models. Furthermore non-dimensional failure mode maps are presented for facesheet compressive failure, core shear failure and global facesheet buckling and wrinkling. Non-dimensional mass of sandwich is incorporated into failure mode maps to enable minimal weight selection. Finally, a simple procedure is proposed to utilize the developed mode maps for optimal design selection of sandwich beams with minimum weight.

5 ACKNOWLEDGEMENT

The authors are grateful for the financial support from the Research and Development Corporation of Newfoundland and Labrador (RDCNL), RDC IgniteR&D contract 5404- 1726-101.

6 REFERENCES

- [1] F. J. Plantema, *Sandwich construction*, Wiley, New York, 1966.
- [2] H. G. Allen, *Analysis and Design of Structural Sandwich Panels: The Commonwealth and International Library: Structures and Solid Body Mechanics Division*, Elsevier, 2013.
- [3] L. A. Carlsson, G. A. Kardomateas, *Structural and failure mechanics of sandwich composites*, Vol. 121, Springer Science & Business Media, 2011.
- [4] K. Niu, R. Talreja, Modeling of wrinkling in sandwich panels under compression, *Journal of Engineering Mechanics* 125 (8) (1999) 875–883.
- [5] A. Mondal, S. Nakhla, Simplified model for the design of composite sandwich construction, in: *Oceans-St. John's*, 2014, IEEE, 2014, pp. 1–12.
- [6] I. Daniel, E. Gdoutos, K.-A. Wang, J. Abot, Failure modes of composite sandwich beams, *International Journal of Damage Mechanics* 11 (4) (2002) 309–334.
- [7] J. Kim, S. R. Swanson, Design of sandwich structures for concentrated loading, *Composite Structures* 52 (3) (2001) 365–373.
- [8] T. McCormack, R. Miller, O. Kesler, L. Gibson, Failure of sandwich beams with metallic foam cores, *International Journal of Solids and Structures* 38 (28) (2001) 4901–4920.
- [9] K. Kabir, T. Vodenitcharova, M. Hoffman, Response of aluminium foam-cored sandwich panels to bending load, *Composites Part B: Engineering* 64 (2014) 24–32.
- [10] A. Petras, M. Sutcliffe, Failure mode maps for honeycomb sandwich panels, *Composite Structures* 44 (4) (1999) 237–252.
- [11] Y. Shenhar, Y. Frostig, E. Altus, Stresses and failure patterns in the bending of sandwich beams with transversely flexible cores and laminated composite skins, *Composite Structures* 35 (2) (1996) 143–152.
- [12] C. A. Steeves, N. A. Fleck, Collapse mechanisms of sandwich beams with composite faces and a foam core, loaded in three-point bending. part i: analytical models and minimum weight design, *International Journal of Mechanical Sciences* 46 (4) (2004) 561–583.
- [13] J. Gere, B. Goodno, *Mechanics of materials*, Nelson Education, 2012.
- [14] P. K. Mallick, *Fiber-reinforced composites: materials, manufacturing, and design*, CRC press, 2007
- [15] S. Chiras, D. Mumm, A. Evans, N. Wicks, J. Hutchinson, K. Dharmasena, H. Wadley, S. Fichter, The structural performance of near-optimized truss core panels, *International Journal of Solids and Structures* 39 (15) (2002) 4093–4115.
- [16] O. A. Bauchau, J. I. Craig, *Structural analysis: with applications to aerospace structures*, Vol. 163, Springer Science & Business Media, 2009